Flexible Solar-Blind Photodetectors Based on β-Ga_2O_3 Films Transferred by a Stamp-Based Printing Technique

Xin Zhou, Ming Li, Jinzhong Zhang, Liyan Shang, Kai Jiang, Yawei Li, Liangqing Zhu, Junhao Chu, and Zhigao Hu

***Abstract*— A stamp-based printing technique was applied to transfer the β-Ga_2O_3 films grown by pulsed laser deposition (PLD) from Si substrates onto some flexible substrates, such as PET, PEN, and PI. It is demonstrated that the β-Ga_2O_3-based flexible solar-blind photodetectors (SBPDs) exhibit brilliant optoelectrical performances with a low dark current of 1.7 pA at 10 V, a I_{254nm}/I_{dark} ratio of 1.2×10^3, rise ($\tau_{r1} = 0.079$ s and $\tau_{r2} = 0.413$ s) and decay ($\tau_{d1} = 0.029$ s and $\tau_{d2} = 0.316$ s) times. In a further step, flexible imaging sensor arrays based on the β-Ga_2O_3/PET were fabricated, which exhibit good imaging capability and resolution. Moreover, wearable UVC-alarms based on the β-Ga_2O_3/PET were realized to monitor the UVC radiation in the environment in real time, which can be used in the COVID-19-related area.**

***Index Terms*— β-Ga_2O_3 films, pulsed laser deposition, stamp-based printing technique, flexible solar-blind photodetectors.**

I. Introduction

ULTRA-VIOLET light can be divided into three regions: UVA (400 nm-320 nm), UVB (320 nm-280 nm) and UVC (280 nm-100 nm) [1]. Among them, the UVC from solar radiation is almost absorbed by the ozone layer and cannot reach the surface of the earth (i.e., solar-blind) [2], [3], [4]. Therefore, solar-blind photodetectors (SBPDs) will not be interfered by sunlight signals, which are widely used in many important fields, such as missile tracking, solar-blind communication system and fire warning [5], [6], [7], [8], [9], [10], [11], [12]. Ga_2O_3 [12], BN [13], [14], [15], diamond [16], [17], AlN [18] GaN [19], [20], and AlGaN [21], [22] are often used to fabricate SBPDs. Among them, Ga_2O_3 has become one of the strong candidates for fabricating SBPDs due to the ultra-wide band gap (~4.9 eV), which is located in the solar-blind spectra. Moreover, Ga_2O_3 has a high chemical/thermal stability and a simple preparation process.

With the rapid spread of the COVID-19, UVC sterilization devices are used to eliminate these viruses. However, continued exposure of UVC will lead to health problems, such as skin damage and retinal damage [3]. It is necessary to monitor UVC radiation in the environment anytime and anywhere to alarm a stranger. However, SBPDs designed on traditional hard substrates (i.e., sapphire, Si) cannot satisfy the new demands, such as wearable, flexible, bendable and portable. Some efforts have been applied to design and fabricate Ga_2O_3-based flexible SBPDs. Amorphous Ga_2O_3 (a-Ga_2O_3) films are often used to fabricate SBPDs on flexible organic subtracts without undergoing a high-temperature process. It is reported that the a-Ga_2O_3 SBPD exhibits a $I_{254\,nm}/I_{dark}$ ratio of up to 4.5×10^4 with a dark current down to 10^{-13} A [23]. The responsivity of the a-Ga_2O_3/ZnO heterojunction photodetectors increases 3.8 times (from 0.65 A/W to 2.49 A/W) and the response time decreases 43% (from 368 ms to 147 ms) by applying a tensile strain of 0.57% on the flexible PET substrates [24].

Unfortunately, the a-Ga_2O_3-based SBPDs always have a high dark current and a long response time due to the defect-related persistent photoconductivity [25]. In order to overcome the challenge, β-Ga_2O_3-based flexible photodetectors have been fabricated [25], [26], [27], [28], [29]. Flexible β-Ga_2O_3 photodetectors on mica substrate demonstrated an excellent performance, including a $I_{254\,nm}/I_{dark}$ ratio larger than 10^6, responsivity of 1.3 A/W and decay speed of 0.026 s [25]. Li *et al.* mechanically exfoliated Ta-doped β-Ga_2O_3 flake from a β-Ga_2O_3 bulk single crystal to fabricate the SBPDs with a high responsivity of 1.32×10^6 A/W, a large detectivity of 5.68×10^{14} Jones and a fast response time of 3.50 ms [26]. However, the size of β-Ga_2O_3 flake is

Manuscript received 4 September 2022; accepted 13 September 2022. Date of publication 16 September 2022; date of current version 24 October 2022. This work was supported in part by the National Natural Science Foundation of China under Grant 62090013, Grant 62074058, Grant 61974043, and Grant 61974044; in part by the National Key Research and Development Program of China under Grant 2019YFB2203403; in part by the Projects of Science and Technology Commission of Shanghai Municipality under Grant 21JC1402100 and Grant 19511120100; and in part by the Program for Professor of Special Appointment (Eastern Scholar), Shanghai Institutions of Higher Learning. The review of this letter was arranged by Editor T.-Y. Seong. *(Corresponding authors: Liangqing Zhu; Zhigao Hu.)*

Xin Zhou, Ming Li, Jinzhong Zhang, Liyan Shang, Kai Jiang, Yawei Li, and Liangqing Zhu are with the Technical Center for Multifunctional Magneto-Optical Spectroscopy (Shanghai) and the Engineering Research Center of Nanophotonics & Advanced Instrument (Ministry of Education), Department of Physics, School of Physics and Electronic Science, East China Normal University, Shanghai 200241, China (e-mail: lqzhu@ee.ecnu.edu.cn).

Junhao Chu and Zhigao Hu are with the Technical Center for Multifunctional Magneto-Optical Spectroscopy (Shanghai) and the Engineering Research Center of Nanophotonics & Advanced Instrument (Ministry of Education), Department of Physics, School of Physics and Electronic Science, East China Normal University, Shanghai 200241, China, and also with the Collaborative Innovation Center of Extreme Optics, Shanxi University, Taiyuan, Shanxi 030006, China (e-mail: zghu@ee.ecnu.edu.cn).

Color versions of one or more figures in this letter are available at https://doi.org/10.1109/LED.2022.3207314.

Digital Object Identifier 10.1109/LED.2022.3207314

small and uncontrollable, which is not suitable for the scale production of Ga_2O_3-based flexible SBPDs.

In this work, β-Ga_2O_3 films with a ($\bar{2}01$)-preferred orientation were grown on Si(100) by pulsed laser deposition (PLD). A stamp-based printing technique is successfully used to transfer the as-deposited β-Ga_2O_3 films from Si substrates onto flexible PET substrates. The β-Ga_2O_3-based flexible SBPDs exhibite a good optoelectronic performance and stability under different bending stresses. In a further step, the flexible imaging sensor arrays (5 × 5) exhibit good imaging capability and resolution. Moreover, wearable UVC-alarms based on the β-Ga_2O_3/PET were fabricated to monitor UVC radiation in the environment for the COVID-19.

II. Experimental

A Ga_2O_3 seed layer was pre-deposited on the Si(100) substrates for 5 min at 500 °C with a partial oxygen pressure of 40 mTorr to avoid the interface stress between Ga_2O_3 films and Si substrates [31]. After that, the oxygen gas was turned off. The sample temperature increased to 750 °C and then maintained for 30 min. Afterward, Ga_2O_3 films were deposited for 60 min at 750 °C with a partial oxygen pressure of 20 mTorr. Then, the as-deposited films had been annealed for 60 min in a vacuum of 10^{-6} Pa without oxygen, the process is shown in Fig. 1(a).

Next, PMMA950K was spin-coated on the Ga_2O_3/Si samples. Hydrofluoric solution (49 mol% HF) was uesd to remove the SiO_2 layer at the interface between the Ga_2O_3 film and Si substrate [32]. Then the peeled films were transferred onto flexible PET substrates following by baking for 5 min at 50 °C, and the PMMA was removed by acetone, as shown in Fig. 1(b). Finally, two-terminal (2 nm/60 nm Ti/Au) SBPDs were fabricated by a thermal evaporator.

The crystalline structure and composition of β-Ga_2O_3 films were analyzed by X-ray diffraction (XRD) and X-ray photoelectron spectroscopy (XPS), respectively. An accurate semiconductor parameter analyzer (Keithley 4200-SCS) was used to probe the optoelectrical performance of the Ga_2O_3-based flexible SBPDs. The UVC light source (254 nm) is produced by a UV quartz tube with a pure UVC filter.

III. Results and Discussion

In Fig. 1c, the X-ray diffraction peaks (⋆) of PET substrates (27° and 56°) are detected in the a-Ga_2O_3/PET and β-Ga_2O_3/PET samples. It suggests that the a-Ga_2O_3 films is amorphous, while the β-Ga_2O_3 films are polycrystalline. For the case of β-Ga_2O_3/Si, there are three peaks nearby 18.9°, 38.4°, and 59.1°, which are corresponding to the ($\bar{2}01$), ($\bar{4}02$), and ($\bar{6}03$) crystal planes of β-Ga_2O_3 (JCPDF Card: No. 43-1012), respectively. For the case of the films transferred from Si onto PET substrates, the widths of the ($\bar{2}01$) peaks become large and the intensities decrease, indicating a smaller average grain size,which is consistent with the AFM results (cf., Fig. 1e and 1f). It indicates that the films were partially etched in the transfer process due to the grain boundary scattering [33]. The XPS spectra indicate that the O/Ga ratio values of the β-Ga_2O_3 films on Si and PET substrates are about 1.50, while that of a-Ga_2O_3 films on PET is about 1.1 (cf., Fig. 1d). It means that there exist many oxygen defects in

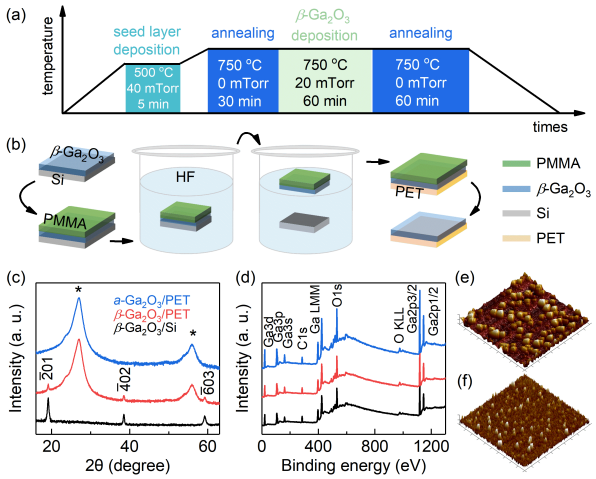

Fig. 1. (a) Schematic diagram of the growth process of β-Ga_2O_3 film on Si(100) substrates by PLD. (b) Schematic flow chart of β-Ga_2O_3 films transferred from Si onto PET substrates. (c) XRD and (d) full XPS spectrum of the β-Ga_2O_3/PET, β-Ga_2O_3/Si and a-Ga_2O_3/PET. AFM images of the β-Ga_2O_3 film (e) before and (f) after transfer (scanning range: 2 μm× 2 μm; hight range: 0 - 25 nm).

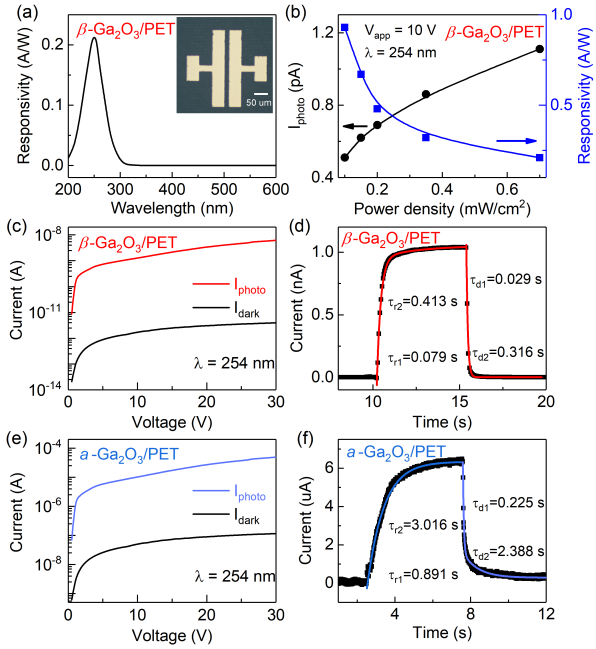

Fig. 2. (a) A response spectrum of a β-Ga_2O_3/PET-based SBPD as a function of illumination wavelength. Inset: microscope photograph of a SBPD. (b) Photocurrent and responsivity of the SBPD as a function of illumination power density (P_{in}). (c) I-V and (d) I-t curves of the β-Ga_2O_3/PET-based flexible SBPD. (e) I-V and (f) I-t curves of the a-Ga_2O_3/PET-based flexible SBPD.

a-Ga_2O_3 films. Therefore, the photogenerated carriers in the a-Ga_2O_3 films are easily captured by these oxygen defects, resulting in a slow response speed [34].

Responsivity (R) of a photodetector is defined as $R = I_{photo}/(P_{in} \times S)$. Here, I_{photo}, P_{in} and S represent the photocurrent, power density of the incident light, and effective working area of the devices, respectively [35]. The response spectrum of a β-Ga_2O_3/PET-based flexible SBPD in Fig. 2a reveals that the response wavelength region is about 200-270 nm, which coincides with the solar-blind region. More carriers are generated as the P_{in} of 254 nm-light increases, leading to a high photocurrent, as shown in Fig. 2b. The

TABLE I
COMPARISON OF THE KEY PARAMETERS OF FLEXIBLE Ga_2O_3 PDS

Active material	Substrate material	I_{dark} (pA)	R (A/W)	Decay time (ms)	Refs.
β-Ga_2O_3	PET	1.7	0.9	90	This work
β-Ga_2O_3	Tape	10^3	40	150	[28]
β-Sn:Ga_2O_3	PI	--	1.18	$>10^3$	[29]
β-Ga_2O_3	Mica	1	1.3	26	[25]
β-Ga_2O_3	Glass fiber	10^3	0.71	190	[27]
β-Ta:Ga_2O_3	PI	10^{-2}	10^8	3	[26]
a-Ga_2O_3	PI	0.1	33.9	90	[23]
a-Ga_2O_3/ZnO	PET	460	2.49	147	[24]
LIG/GaO_x	PI	10^3	0.043	60	[30]

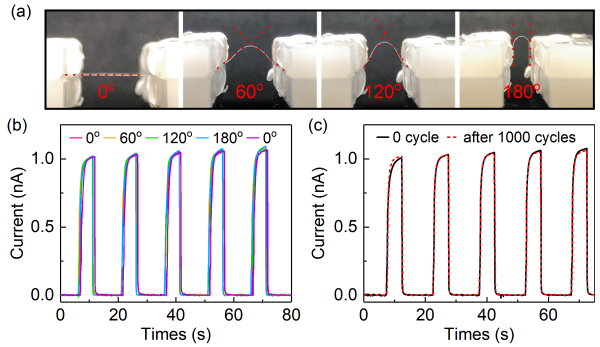

Fig. 3. (a) Photographs of a β-Ga_2O_3/PET-based flexible SBPD with the various bending angles of 0, 60, 120, and 180°. I-t curves of the device at 10 V (b) with different bending angles and (c) without bending and after 1000 bending cycles.

responsivity of SBPD in Fig. 2b decreases with increasing the P_{in} since the photocurrent tends to be saturated. In Fig. 2c, the β-Ga_2O_3-based flexible SBPDs have a low dark current (I_{dark}) of 1.7 pA at 10 V and a $I_{254\ nm}/I_{dark}$ ratio of 1.2×10^3. The UVC light pulse with a period of 5 s was applied to the device to probe the response times, as depicted in Fig. 2d. The I-t curves were fitted by the biexponential relationship [18]: $I = I_0 + Ae^{-t/\tau_1} + Be^{-t/\tau_2}$. Here, I_0 is the photocurrent at the steady state, A and B are fitting constants, and τ_1 and τ_2 are the relaxation times of the fast and slow response components of the rise/decay edges, respectively. The SBPDs based on β-Ga_2O_3 films have a fast response with rise ($\tau_{r1} = 0.079$ s and $\tau_{r2} = 0.413$ s) and decay ($\tau_{d1} = 0.029$ s and $\tau_{d2} = 0.316$ s) times.

For comparison, a-Ga_2O_3 films on PET substrates were deposited by PLD at room temperature under the same partial oxygen pressure of 20 mTorr. The corresponding photoelectronic responses are presented in Figs. 2e and 2f. The I_{photo} and I_{dark} of a-Ga_2O_3-based flexible SBPDs are larger than those of the β-Ga_2O_3-based ones due to the more oxygen vacancies in the a-Ga_2O_3 films [34]. The corresponding response time ($\tau_{d2} = 0.316$ s) of the β-Ga_2O_3 based photodetectors is much shorter than that of a-Ga_2O_3 ($\tau_{d2} = 2.388$ s) due to the persistent photoconductivity effect [25]. Table I shows a comparison of our work with some other Ga_2O_3-based flexible SBPDs [23], [24], [25], [26], [27], [28], [29], [30].

The optoelectronic properties of the β-Ga_2O_3-based flexible SBPDs at the various bending states (the corresponding strain: 0%, 0.17%, 0.23% and 0.38%) are investigated as shown in Fig. 3. The I-t curves are essentially coincident at different bending angles, which indicates that the effect of bending

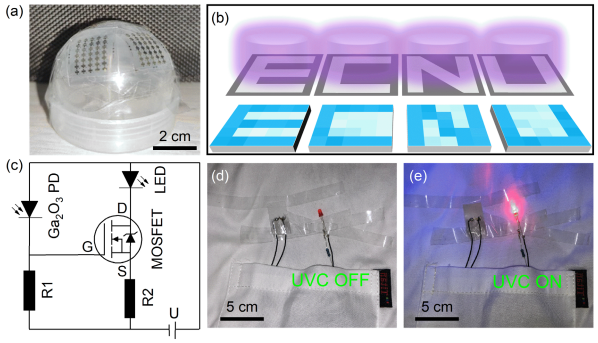

Fig. 4. (a) Photograph of the flexible imaging sensor arrays. (b) The bottom figures "ECNU" show the corresponding images acquired from the sensor arrays under the UVC illumination through the above photomasks. (c) The circuit of wearable UVC-alarms based on the β-Ga_2O_3/PET PD and the corresponding photographs on clothes when UVC (d) OFF and (e) ON.

stress can be ignored. Moreover, no obvious optoelectronic performance degradation is observed after 1000 bending cycles in Fig. 3c. The results reveal that the flexible β-Ga_2O_3-based SBPDs have excellent stability and reliability.

In a further step, flexible solar-blind imaging sensor arrays were fabricated consisting of an array cell of 5×5 β-Ga_2O_3-based flexible SBPDs. The sensor arrays were stuck to a 5 cm-diameter hemisphere, as shown in Fig. 4a. In Fig. 4b, the photomasks "ECNU" were placed above the flexible imaging sensor arrays. Under the UVC illumination (254 nm), the corresponding optical pattern is generated on the flexible imaging sensors. The unshaded areas have high photocurrent, while shaded areas have low dark currents. Note that the output currents of each SBPD unit from low to high corresponds to different colors from white to blue. The "ECNU" pattern can be clearly detected, which means that the flexible imaging sensor arrays have excellent imaging capability and resolution.

Wearable UVC alarms based on β-Ga_2O_3/PET were fabricated to monitor UVC radiation, which can be used in the COVID-19-related area. The corresponding circuit is shown in Fig. 4c. When UVC light is OFF, the resistance of the SBPD is large. The gate voltage of the MOSFET is lower than the threshold voltage (2 V). Therefore, the MOSFET is in the off state, and the LED does not work, as shown in Fig. 4d. On the contrary, the SBPD resistance decreases suddenly when the UVC light is ON. The MOSFET is in the on state and the LED works (cf., Fig. 4e).

IV. CONCLUSION

In summary, β-Ga_2O_3 films have been deposited on Si(100) substrates by PLD. The as-deposited films were transferred from Si onto PET substrates by the stamp-based printing technique. The flexible SBPDs based on the β-Ga_2O_3/PET exhibit an optimum optoelectrical performance with a low dark current of 1.7 pA at 10 V, a high $I_{254\ nm}/I_{dark}$ ratio of 1.2×10^3, rise ($\tau_{r1} = 0.079$ s and $\tau_{r2} = 0.413$ s) and decay ($\tau_{d1} = 0.029$ s and $\tau_{d2} = 0.316$ s) times, and good stability and repeatability under bending stress. Finally, flexible imaging sensor arrays and wearable UVC-alarms were realized, which demonstrate the practical applications of β-Ga_2O_3-based flexible SBPDs in the fields of solar-blind photodetection.

REFERENCES

[1] J. Yang, K. Liu, X. Chen, and D. Shen, "Recent advances in optoelectronic and microelectronic devices based on ultrawide-bandgap semiconductors," *Prog. Quantum Electron.*, vol. 83, May 2022, Art. no. 100397, doi: 10.1016/j.pquantelec.2022.100397.

[2] P. V. K. Yadav, B. Ajitha, Y. A. Kumar Reddy, and A. Sreedhar, "Recent advances in development of nanostructured photodetectors from ultraviolet to infrared region: A review," *Chemosphere*, vol. 279, Sep. 2021, Art. no. 130473, doi: 10.1016/j.chemosphere.2021.130473.

[3] U. Varshney, N. Aggarwal, and G. Gupta, "Current advances in solar-blind photodetection technology: Using Ga_2O_3 and AlGaN," *J. Mater. Chem. C*, vol. 10, p. 1573, Feb. 2022, doi: 10.1039/d1tc05101f.

[4] M. F. Al Fattah, A. A. Khan, H. Anabestani, M. M. Rana, S. Rassel, J. Therrien, and D. Ban, "Sensing of ultraviolet light: A transition from conventional to self-powered photodetector," *Nanoscale*, vol. 13, no. 37, pp. 15526–15551, Oct. 2021, doi: 10.1039/d1nr04561j.

[5] Q. Cai, H. You, H. Guo, J. Wang, B. Liu, Z. Xie, D. Chen, H. Lu, Y. Zheng, and R. Zhang, "Progress on AlGaN-based solar-blind ultraviolet photodetectors and focal plane arrays," *Light: Sci. Appl.*, vol. 10, no. 1, p. 94, Apr. 2021, doi: 10.1038/s41377-021-00527-4.

[6] D. Kaur and M. Kumar, "A strategic review on gallium oxide based deep-ultraviolet photodetectors: Recent progress and future prospects," *Adv. Opt. Mater.*, vol. 9, no. 9, May 2021, Art. no. 2002160, doi: 10.1002/ADOM.202002160.

[7] B. Liu, D. Chen, H. Lu, T. Tao, Z. Zhuang, Z. Shao, W. Xu, H. Ge, T. Zhi, F. Ren, J. Ye, Z. Xie, and R. Zhang, "Hybrid light emitters and UV solar-blind avalanche photodiodes based on III-nitride semiconductors," *Adv. Mater.*, vol. 32, no. 27, Oct. 2019, Art. no. 1904354, doi: 10.1002/ADMA.201904354.

[8] S. Maity, K. Sarkar, and P. Kumar, "A progressive journey into 2D-chalcogenide/carbide/nitride-based broadband photodetectors: Recent developments and future perspectives," *J. Mater. Chem. C*, vol. 9, no. 41, pp. 14532–14572, Oct. 2021, doi: 10.1039/d1tc02820k.

[9] A. K. Saikumar, S. D. Nehate, and K. B. Sundaram, "A review of recent developments in aluminum gallium oxide thin films and devices," *Crit. Rev. Solid State Mater. Sci.*, vol. 47, no. 4, pp. 538–569, Jul. 2022, doi: 10.1080/10408436.2021.1922357.

[10] C. Xie, X. Lu, X. Tong, Z. Zhang, F. Liang, L. Liang, L. Luo, and Y. Wu, "Recent progress in solar-blind deep-ultraviolet photodetectors based on inorganic ultrawide bandgap semiconductors," *Adv. Funct. Mater.*, vol. 29, no. 9, Feb. 2019, Art. no. 1806006, doi: 10.1002/ADFM.201806006.

[11] C. Wu, F. Wu, C. Ma, S. Li, A. Liu, X. Yang, Y. Chen, J. Wang, and D. Guo, "A general strategy to ultrasensitive Ga_2O_3 based self-powered solar-blind photodetectors," *Mater. Today Phys.*, vol. 23, Mar. 2022, Art. no. 100643, doi: 10.1016/j.mtphys.2022.100643.

[12] Y. Chen, Y. Lu, X. Yang, S. Li, K. Li, X. Chen, Z. Xu, J. Zang, and C. Shan, "Bandgap engineering of Gallium oxides by crystalline disorder," *Mater. Today Phys.*, vol. 18, May 2021, Art. no. 100369, doi: 10.1016/j.mtphys.2021.100369.

[13] J. Chen, G. Wang, J. Meng, Y. Cheng, Z. Yin, Y. Tian, J. Huang, S. Zhang, J. Wu, and X. Zhang, "Low-temperature direct growth of few-layer hexagonal boron nitride on catalyst-free sapphire substrates," *ACS Appl. Mater. Interfacts*, vol. 14, no. 5, pp. 7004–7011, Jan. 2022, doi: 10.1021/ACSAMI.1c22626.

[14] X. Zhu, L. Chen, X. Tang, H. Wang, Y. Xiao, W. Gao, and H. Yin, "Plasmonic enhancement in deep ultraviolet photoresponse of hexagonal boron nitride thin films," *Appl. Phys. Lett.*, vol. 120, no. 9, Feb. 2022, Art. no. 091109, doi: 10.1063/5.0081117.

[15] S. Kaushik, S. Karmakar, R. K. Varshney, H. Sheoran, D. Chugh, C. Jagadish, H. H. Tan, and R. Singh, "Deep-ultraviolet photodetectors based on hexagonal boron nitride nanosheets enhanced by localized surface plasmon resonance in Al nanoparticles," *ACS Appl. Nano Mater.*, vol. 5, no. 5, pp. 7481–7491, May 2022, doi: 10.1021/acsanm.2c01466.

[16] M. Girolami, V. Serpente, M. Mastellone, M. Tardocchi, M. Rebai, Q. Xiu, J. Liu, Z. Sun, Y. Zhao, V. Valentini, and D. M. Trucchi, "Self-powered solar-blind ultrafast UV-C diamond detectors with asymmetric Schottky contacts," *Carbon*, vol. 189, pp. 27–36, Apr. 2022, doi: 10.1016/j.carbon.2021.12.050.

[17] Z.-F. Zhang, C.-N. Lin, X. Yang, J.-H. Zang, K.-Y. Li, Y.-C. Lu, Y.-Z. Li, L. Dong, and C.-X. Shan, "Wafer-sized polycrystalline diamond photodetector planar arrays for solar-blind imaging," *J. Mater. Chem. C*, vol. 10, no. 16, pp. 6488–6496, Apr. 2022, doi: 10.1039/d2tc00327a.

[18] N. Liu, T. Zhang, L. Chen, J. Zhang, S. Hu, W. Guo, W. Zhang, and J. Ye, "Fast-response amorphous Ga_2O_3 solar-blind ultraviolet photodetectors tuned by a polar AlN template," *IEEE Electron Device Lett.*, vol. 43, no. 1, pp. 68–71, Jan. 2022, doi: 10.1109/LED.2021.3132497.

[19] B. Uppalapati, D. Gajula, F. Bayram, A. Kota, A. Gunn, D. Khan, V. P. Chodavarapu, and G. Koley, "An AlGaN/GaN dual channel triangular microcantilever based UV detector," *ACS Photon.*, vol. 9, no. 6, pp. 1908–1918, Jun. 2022, doi: 10.1021/acsphotonics.1c01316.

[20] P.-F. Chi, F.-W. Lin, M.-L. Lee, and J.-K. Sheu, "High-responsivity solar-blind photodetectors formed by Ga_2O_3/p-GaN bipolar heterojunctions," *ACS Photon.*, vol. 9, no. 3, pp. 1002–1007, Mar. 2022, doi: 10.1021/acsphotonics.1c01892.

[21] Q. Wen, C. Wang, X. Qiu, Z. Lv, and H. Jiang, "Significant performance improvement of AlGaN solar-blind heterojunction phototransistors by using Na_2S solution based surface treatment," *Appl. Surf. Sci.*, vol. 591, Jul. 2022, Art. no. 153144, doi: 10.1016/j.apsusc.2022.153144.

[22] Y. Gao, J. Yang, X. Ji, R. He, J. Yan, J. Wang, and T. Wei, "Semipolar (11$\bar{2}$2) AlGaN-based solar-blind ultraviolet photodetectors with fast response," *ACS Appl. Mater. Interfaces*, vol. 14, no. 18, pp. 21232–21241, Apr. 2022, doi: 10.1021/acsami.2c03636.

[23] Y. Yang, W. Liu, T. Huang, M. Qiu, R. Zhang, W. Yang, J. He, X. Chen, and N. Dai, "Low deposition temperature amorphous ALD-Ga_2O_3 thin films and decoration with MoS_2 multilayers toward flexible solar-blind photodetectors," *ACS Appl. Mater. Interfaces*, vol. 13, no. 35, pp. 41802–41809, Sep. 2021, doi: 10.1021/ACSAMI.1c11692.

[24] H. Wang, J. Ma, L. Cong, H. Zhou, P. Li, L. Fei, B. Li, H. Xu, and Y. Liu, "Piezoelectric effect enhanced flexible UV photodetector based on Ga_2O_3/ZnO heterojunction," *Mater. Today Phys.*, vol. 20, Sep. 2021, Art. no. 100464, doi: 10.1016/j.mtphys.2021.100464.

[25] M. Ding, K. Liang, S. Yu, X. Zhao, H. Ren, B. Zhu, X. Hou, Z. Wang, P. Tan, H. Huang, Z. Zhang, X. Ma, G. Xu, and S. Long, "Aqueous-printed Ga_2O_3 films for high-performance flexible and heat-resistant deep ultraviolet photodetector and array," *Adv. Opt. Mater.*, vol. 10, no. 16, Aug. 2022, Art. no. 2200512, doi: 10.1002/ADOM.202200512.

[26] X.-X. Li, G. Zeng, Y.-C. Li, H. Zhang, Z.-G. Ji, Y.-G. Yang, M. Luo, W.-D. Hu, D. W. Zhang, and H.-L. Lu, "High responsivity and flexible deep-UV phototransistor based on Ta-doped β-Ga_2O_3," *npj Flexible Electron.*, vol. 6, no. 1, p. 47, Jun. 2022, doi: 10.1038/s41528-022-00179-3.

[27] S. Wang, H. Sun, Z. Wang, X. Zeng, G. Ungar, D. Guo, J. Shen, P. Li, A. Liu, C. Li, and W. Tang, "*In situ* synthesis of monoclinic β-Ga_2O_3 nanowires on flexible substrate and solar-blind photodetector," *J. Alloys Compounds*, vol. 787, pp. 133–139, May 2019, doi: 10.1016/j.jallcom.2019.02.031.

[28] X. Tang, K. H. Li, Y. Zhao, Y. Sui, H. Liang, Z. Liu, C. H. Liao, W. Babatain, R. Lin, C. Wang, Y. Lu, F. S. Alqatari, Z. Mei, W. Tang, and X. Li, "Quasi-epitaxial growth of beta-Ga_2O_3-coated wide band gap semiconductor tape for flexible UV photodetectors," *ACS Appl. Mater. Interfaces*, vol. 14, p. 1304, Dec. 2021, doi: 10.1021/acsami.1c15560.

[29] J. Lai, M. N. Hasan, E. Swinnich, Z. Tang, S.-H. Shin, M. Kim, P. Zhang, and J.-H. Seo, "Flexible crystalline β-Ga_2O_3 solar-blind photodetectors," *J. Mater. Chem. C*, vol. 8, no. 42, pp. 14732–14739, Nov. 2020, doi: 10.1039/d0tc03740k.

[30] C. Wu, F. Wu, H. Hu, C. Ma, J. Ye, S. Wang, H. Wu, J. Wang, A. Liu, and D. Guo, "Work function tunable laser induced graphene electrodes for Schottky type solar-blind photodetectors," *Appl. Phys. Lett.*, vol. 120, no. 10, Mar. 2022, Art. no. 101102, doi: 10.1063/5.0080855.

[31] K. Gu, Z. Zhang, K. Tang, J. Huang, Y. Shang, Y. Shen, M. Liao, and L. Wang, "Effect of a seed layer on microstructure and electrical properties of Ga_2O_3 films on variously oriented Si substrates," *Vacuum*, vol. 195, Jan. 2022, Art. no. 110671, doi: 10.1016/j.vacuum.2021.110671.

[32] Y. Liu, L. Wang, Y. Zhang, X. Dong, X. Sun, Z. Hao, Y. Luo, C. Sun, Y. Han, B. Xiong, J. Wang, and H. Li, "Demonstration of n-Ga_2O_3/p-GaN diodes by wet-etching lift-off and transfer-print technique," *IEEE Electron Device Lett.*, vol. 42, no. 4, pp. 509–512, Apr. 2021, doi: 10.1109/LED.2021.3056445.

[33] S.-L. Ou, D.-S. Wuu, Y.-C. Fu, S.-P. Liu, R.-H. Horng, L. Liu, and Z.-C. Feng, "Growth and etching characteristics of gallium oxide thin films by pulsed laser deposition," *Mater. Chem. Phys.*, vol. 133, nos. 2–3, pp. 700–705, Apr. 2012, doi: 10.1016/j.matchemphys.2012.01.060.

[34] X. Zhou, M. Li, J. Zhang, L. Shang, K. Jiang, Y. Li, L. Zhu, Z. Hu, and J. Chu, "High quality P-type MG-doped β-Ga_2O_3-δ films for solar-blind photodetectors," *IEEE Electron Device Lett.*, vol. 43, no. 4, pp. 580–583, Apr. 2022, doi: 10.1109/LED.2022.3151476.

[35] Y. Wang, R. Fu, Y. Wang, B. Li, H. Xu, A. Shen, and Y. Liu, "A high responsivity self-powered solar-blind DUV photodetector based on a nitrogen-doped graphene/β-Ga_2O_3 microwire p–n heterojunction," *IEEE Electron Device Lett.*, vol. 43, no. 7, pp. 1073–1076, Jul. 2022, doi: 10.1109/LED.2022.3172728.